

Jimmy Baert,
Florentin Langouche^a,
Peter Van Puyvelde^b

Department of Chemical Engineering,
Katholieke Universiteit Leuven,
Leuven, Belgium
e-mail: jimmy.baert@cit.kuleuven.be

^a Solvay Central Laboratory,
Neder Over Heembeek,
Brussels, Belgium
e-mail: florentin.langouche@solvay.com

^b Department of Chemical Engineering,
Katholieke Universiteit Leuven,
Leuven, Belgium
e-mail: peter.vanpuyvelde@cit.kuleuven.be

Flow-induced Crystallization of PB-1: Characterizing the Onset of Shish-kebab Formation

Abstract

In this work, it is shown that optical techniques, more specifically birefringence and transmitted intensity measurements, provide an excellent tool to characterize the transition to highly anisotropic structures in polymer crystallization for shear rates close to industrial processing conditions. This is illustrated for the flow-induced crystallization of isotactic poly-1-butene (PB-1). A characteristic upturn in the flow birefringence and a sharp increase in crystallization kinetics both indicate the onset of the formation of shish-kebab structures with an increased level of molecular orientation. Moreover, the results indicate that this transition is strongly molecular weight (M_w) dependent.

Key words: birefringence, transmitted intensity, flow-induced crystallization, shish kebab.

thermal histories and the semi-crystalline materials will crystallize after or even during flow. The morphology of the final product, and as a result its properties and quality, depend on the manner in which the polymer crystallizes from the flowing melt, and will hence be affected by both the thermal and the mechanical history that the polymer experiences in the molten state.

In the last few decades, there have been several investigations into the route by which a polymer melt, subjected to flow and a certain degree of undercooling, transforms into a crystalline state (see for instance a recent review by Kumaraswamy [1]). As a result, we are beginning to gain insight into the molecular characteristics that control the crystallization pathways adopted by a stressed polymer melt. For example, it is now well known that the application of shear flow to an undercooled polymer melt enhances the crystallization process, mainly through an increase in nucleation [2-12], the extent of which depends on many factors, such as the processing parameters and the molecular properties of the polymer. Although one of the primary challenges in the study of shear-induced crystallization was to develop experimental methods that allow conditions close to those encountered in real processing situations, many of the reported results have been obtained in the low shear rate region, using either rheometrical equipment [13-15] or using commercial shear cells like, for instance, the Linkam cell CSS-450 [16-19]. Experimental results extending into the high shear rate region are much more limited. The research groups of Janeschitz-Kriegl [20-24] and Kornfield [2, 25, 26] used a short-time

shearing protocol in combination with an extrusion die to study the effects of intense shear flow. However, a major drawback of these extrusion die set-ups is the non-homogeneous character of the flow field throughout the sample, resulting in optical signals that are dominated by structure formation near the die walls. Recently, a sandwich-type shear cell that can be operated from the low shear rate region up to rates that generate a highly oriented structure was developed and used to study the flow-induced crystallization of i-PP [27] and PB-1 [28]. The advantage of this shear cell is that it imposes a homogeneous shear flow, resulting in a constant shear rate throughout the entire sample. Hence, the optical signals are not dominated by structure formation near the walls.

In the present paper, the characterization of the formation of highly oriented structures at high shear rates and the effect of M_w on this formation is discussed for the flow-induced crystallization of two PB-1 samples with a different M_w . The previously mentioned sandwich-type cell enabled us to access the high shear rate region where highly oriented structures develop. In polymer science, these highly anisotropic structures are often called shish kebabs, due to their typical crystalline assembly consisting of a central core fibre (the shish) and chain-folded lamellae (the kebabs) perpendicular to it. The structural features of these shish-kebab crystals provide one of the routes for the development of high strength-high modulus fibres [29]. In the melt spinning sector, for example, detailed control of crystallization and orientation can be used to provide fibres with very different strengths, stiffnesses, and dyeabilities. Also in this

Introduction

The crystallization of flowing polymer melts is of immense technological relevance to polymer processing. Semi-crystalline polymers comprise nearly two-thirds of all synthetic polymers and they are processed to form films, fibres, and moulded articles using operations such as extrusion, injection moulding, fibre spinning, film blowing, etc. During this processing, molten polymers are subjected to strong deformations and complex

paper, the effect of M_w has been studied because understanding the role of the molecular structure in polymer crystallization under processing conditions is essential in controlling the morphology and end properties of polymer products. The obtained knowledge can then be applied to tailor properties (e.g. stiffness, toughness, optical properties) for particular application requirements by adjusting the processing parameters and/or molecular properties.

Experimental section

Materials

The two isotactic PB-1s (PB0400 and PB0800) used in this study are commercial grades provided by Basell Polyolefins in the form of pellets. Both grades have an isotacticity of 98.8% and contain no nucleating agents. PB0400 has an $M_w = 176$ kg/mol and a polydispersity of 5.7; PB0800 has an $M_w = 133$ kg/mol and a polydispersity of 4.3 (data obtained from GPC measurements by Basell Polyolefins). More material properties and a rheological characterization can be found in previous publications [12, 28].

Methods

For the experiments, a shear cell [27, 28] developed at the Solvay Central Laboratory was used. It is a small sandwich-type cell in which the sample is uniaxially sheared between two oppositely moving glass windows, driven by a servomotor. The glass windows of the cell are incorporated in sample holders that are placed in independently heated conditioning blocks. The typical thickness of a sheared

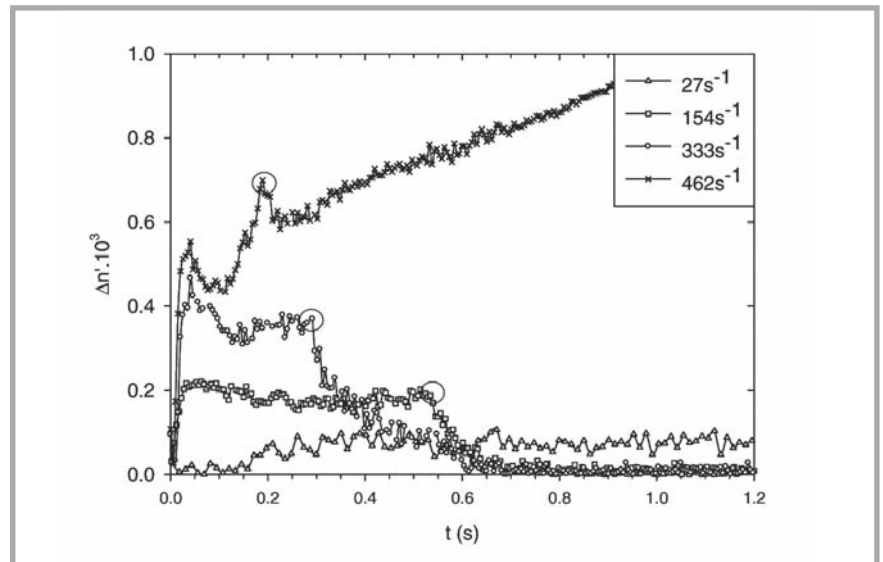


Figure 1. Flow birefringence of PB0400 ($T_c = 98$ °C and $\gamma = 100$). The circles indicate the end of each shear pulse.

sample is 50-100 μm . The shear cell can be operated from the low shear rate region up to rates of 1500 s^{-1} and deformations up to a few hundred shear units can be achieved. The main advantage of this shear cell is that the probed structure is homogeneous, i.e. there is a constant shear rate throughout the entire sample, which is not the case for the extrusion die configurations that have been used up to now [2, 20-26].

Windows and holes are provided in the equipment to view the flow-vorticity plane of the sheared sample. An optical train consisting of a modulated laser allows the transmitted intensity I_{dc} and the birefringence $\Delta n'$ to be followed during shear flow and subsequent crystallization. The birefringence during shear is related

to the anisotropy in the conformation of polymer chains, whereas the transmitted intensity and the birefringence after the onset of crystallization arise due to scattering from crystallites and are sensitive to the size, shape, and anisotropy of the crystallites. The birefringence $\Delta n'$ is obtained from:

$$\Delta n' = \frac{\lambda \delta'}{2\pi e} \quad (1)$$

Here, e is the sample thickness, λ the laser wavelength (670 nm), and δ' the optical retardation calculated from:

$$|\sin \delta'| = \frac{\sqrt{I_{\sin}^2 + I_{\cos}^2}}{I_{dc}} \quad (2)$$

with I_{\sin} and I_{\cos} the amplitudes of a particular sine and cosine component in the detected laser beam [27].

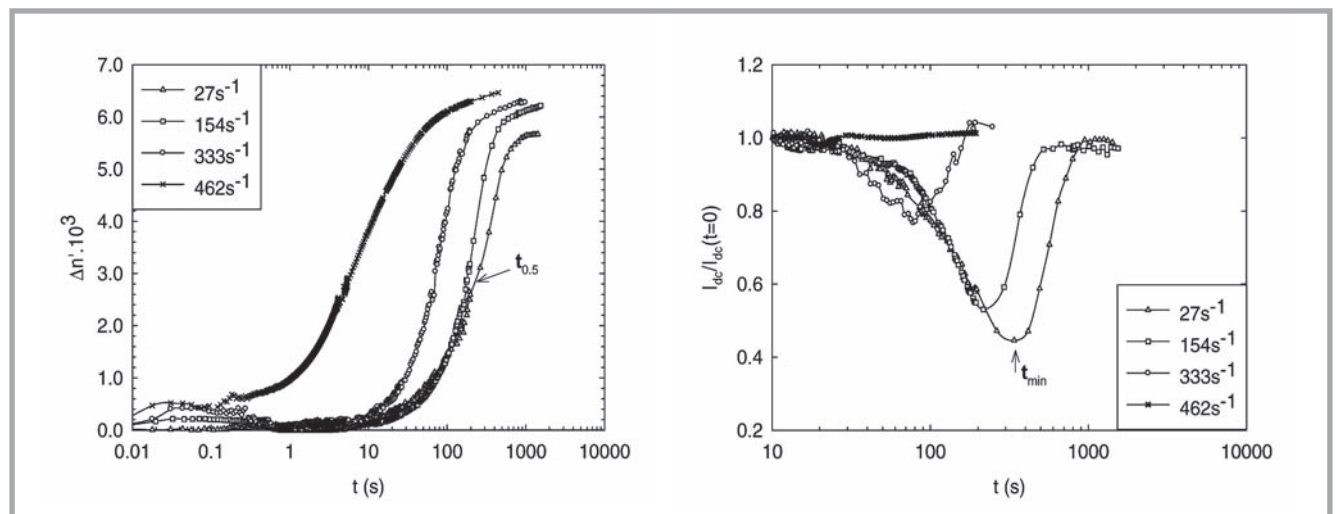


Figure 2. The evolution of birefringence (left) and transmitted intensity (right) during the isothermal crystallization of PB0400 after shearing with different shear rates ($T_c = 98$ °C and $\gamma = 100$).

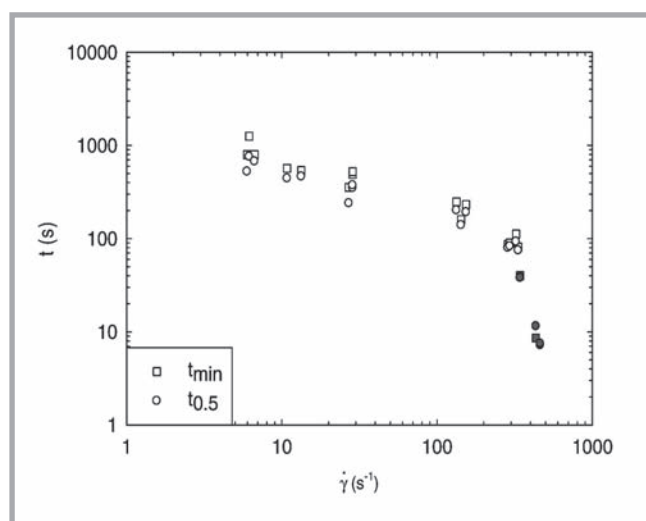


Figure 3. Characteristic crystallization times as a function of shear rate ($T_c = 98\text{ }^\circ\text{C}$ and $\gamma = 100$). The presence of the characteristic upturn in the flow birefringence is indicated by grey symbols.

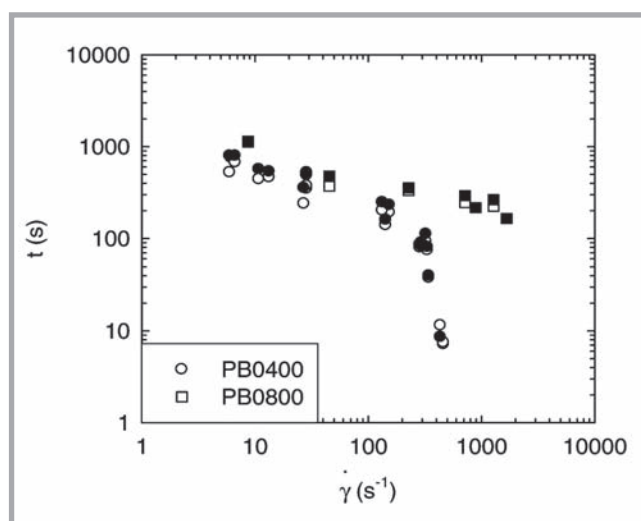


Figure 4. Crystallization times $t_{0.5}$ (empty symbols) and t_{min} (filled symbols) as a function of shear rate for two samples with a different M_w ($T_c = 98\text{ }^\circ\text{C}$ and $\gamma = 100$).

To erase the thermal and flow history, the samples were always annealed at $200\text{ }^\circ\text{C}$ for 10 minutes in a separate oven. Subsequently, they were cooled to $150\text{ }^\circ\text{C}$ and transferred to the conditioning blocks kept at the desired crystallization temperature T_c . This procedure avoids long cooling times typical of the already mentioned extrusion die configurations [2, 20-26]. The thermal characteristics of the set-up resulted in a time of about 10 minutes to quench the sample to the measurement temperature. For the experiments, a zero time scale was assigned to the start of the shear flow, corresponding to the instant at which the crystallization temperature T_c was reached. In all the experiments, the transmitted laser light was measured during shear flow and subsequent isothermal crystallization. More details on the construction, the temperature control and the limitations of the apparatus, the optical set-up, and the calculation of the birefringence can be found in references 27 and 28.

Results and discussion

Characterizing the formation of the shish-kebab structure

The use of the sandwich-type shear cell in combination with the optical set-up described in the previous section provides different ways to detect the formation of the highly anisotropic shish-kebab structure [27, 28]. A first indication is the presence of an unusual upturn in the flow birefringence, the term commonly used to indicate the development of birefringence during flow. In their extrusion die experiments, Kumaraswamy et al.

[2, 25] pointed out the presence of such an upturn above a critical shear stress and strain and attributed this to a change in the crystallization mechanism, i.e. the formation of a 'shear-induced structure' related to the presence of oriented precursors. A similar upturn was observed at high shear rates for experiments on i-PP [27] and PB-1 [28] using the sandwich-type cell. In **Figure 1**, the birefringence of PB0400 during the short flow pulse is plotted for different shear rates $\dot{\gamma}$ ($T_c = 98\text{ }^\circ\text{C}$ and $\gamma = 100$). The instant at which the shear flow is stopped is indicated by circles. The curves show the typical behaviour previously described in the literature [2, 25, 27, 28]: a slight overshoot stabilizing to a plateau level (related to the level of molecular orientation) followed by a relaxation. However, for the highest shear rate shown, $\dot{\gamma} = 462\text{ s}^{-1}$, there is an unusual upturn in the flow birefringence curve and the birefringence hardly relaxes after the cessation of the flow, indicating the formation of shish-kebab structures.

A second indication of the formation of the shish-kebab structure is the sharp increase in the crystallization kinetics. In **Figure 2**, the birefringence (left) and transmitted intensity (right) are monitored during the isothermal crystallization of PB0400 ($T_c = 98\text{ }^\circ\text{C}$ and $\gamma = 100$), again showing the typical behaviour [27, 28]. The time needed to reach 50% of the maximum of the birefringence, defined as $t_{0.5}$, and the instant for which the intensity reaches its minimum, defined as t_{min} , were used to determine the crystallization kinetics qualitatively. Both char-

acteristic times are indicated in **Figure 2** for $\dot{\gamma} = 27\text{ s}^{-1}$. With increasing shear rate, the time needed for the crystalline orientation to become visible in the birefringence signal and the time for the intensity to reach a minimum value both decrease. These are indications of the faster crystallization kinetics.

In **Figure 3**, both characteristic time scales for the crystallization kinetics of PB0400, $t_{0.5}$ and t_{min} , are plotted as a function of the shear rate ($T_c = 98\text{ }^\circ\text{C}$ and $\gamma = 100$). As was shown in previous studies [27, 28], there is a good quantitative agreement between the crystallization times. The obvious change in the slope of these curves at higher shear rates corresponds to the characteristic upturn in flow birefringence (for which the presence is indicated by grey symbols in **Figure 3**), and thus with the onset of the highly anisotropic structure formation.

Although not discussed here, it should be mentioned that, very recently, Mykhaylyk et al. [30] showed that for blends of hydrogenated polybutadienes the specific work of flow also provides a criterion for the formation of shish kebabs. According to these authors, the magnitude of the specific work required to create shish-kebab structures depends on both the chemical structure of the polymer and its molecular weight distribution.

Effect of molecular weight

The M_w plays a critical role in the flow-induced crystallization of polymers be-

cause the length of the polymer chains largely determines their dynamics and their orientation state during shear. Since the relaxation time of the polymer chains is proportional to the molecular weight, long chains would possess much longer relaxation times than short chains. As a result, long polymer chains may not have sufficient time to relax back to the random coil configuration after the cessation of flow and would remain in the stretched state, whereas short chains can quickly relax back to the coiled state without a preferred orientation. It is this molecular orientation that mediates the pathway to nucleation and anisotropic structure formation.

In **Figure 4** (see page 75), the crystallization times obtained from birefringence and transmission measurements, $t_{0.5}$ and t_{min} , are plotted as a function of shear rate for both PB0400 and PB0800. Whereas the curve for PB0400 shows a sharp increase in crystallization kinetics at high shear rates, related to the presence of shish-kebab structures, this is not the case for the low M_w PB0800. The relaxation time of these chains is too short to form threadlike precursors, even for the highest applicable shear rate of 1500 s^{-1} .

According to the classification of flow-induced crystallization by van Meerveld et al. [31], the transition from an enhanced nucleation rate of spherulites towards the development of the shish-kebab structure correlates with the transition from the orientation of the chain segments to the rotational isomerization of the high- M_w chains in the melt, which only occurs for $De_s > 1$ and $\lambda > \lambda^*(T)$. The Deborah number De_s is defined as $De_s = \tau_s \dot{\gamma}$, with τ_s the time scale associated with chain stretching and retraction, and $\dot{\gamma}$ the shear rate. The stretch ratio λ is defined as $\lambda = L/L_0$, the ratio of the current length of the contour path of the polymer chain, L , to the equilibrium value L_0 . At large λ , the chain configuration becomes non-Gaussian and the amount of rotational isomerization is large. The parameter λ^* denotes the transition between these two chain-stretching regimes, which may be identified as weak and strong stretching conditions, respectively.

Calculating the characteristic Deborah number corresponding to the transition to the highly oriented regime in flow-induced crystallization of PB0400 results in $De_s \approx 35$. This value corresponds rather well to the results on i-PP presented

by van Meerveld et al. [31] and Vega et al. [32]. It is assumed that PB0800 will display this transition to shish-kebab structures for the same value of the Deborah number as is the case for PB0400, i.e. $De_s \approx 35$. Since both polymers were investigated under the same conditions ($T_c = 98 \text{ }^\circ\text{C}$ and $\gamma = 100$) and have a similar polydispersity, the assumption that the onset of chain stretching can be related to a single universal magnitude for De_s is not unreasonable [31]. For PB0800, this results in a critical shear rate of approximately 1800 s^{-1} and from **Figure 4** it can be seen that this is a plausible value. Thus, it is expected that, with increasing shear rate, a sharp acceleration of the crystallization and a characteristic upturn in flow birefringence will eventually occur even for the low M_w sample. However, since this shear rate is beyond the limit of the shearing cell, the onset of shish-kebab formation could not be checked experimentally.

Conclusion

The use of a sandwich-type shear cell that can be operated up to shear rates of 1500 s^{-1} in combination with a modulated laser made it possible to identify the transition to shish-kebab structures in flow-induced crystallization of two isotactic PB-1 samples with a different M_w . At high shear rates, there is a sharp rise in birefringence accompanied by a characteristic upturn in the birefringence pattern during flow, typical of the formation of shear-induced structures. Curves displaying the crystallization kinetics as a function of shear rate, based on characteristic crystallization times from birefringence and intensity measurements, display a sharp change in slope occurring nearly together with the characteristic upturn in the flow birefringence. Furthermore, it has been shown that M_w plays an important role in this transition to a highly anisotropic structure, since the chain length strongly affects the state of orientation of the polymer chains.

References

1. Kumaraswamy G.J.; *Macromol. Sci. Polym. Rev.* 2005, 45, 375-397.
2. Kumaraswamy G., Issaian A., Kornfield J.A.; *Macromolecules* 1999, 32, 7537-7547.
3. Bove L., Nobile M.R.; *Macromol. Symp.* 2002, 185, 135-147.
5. Tribout C., Monasse B., Haudin J.M.; *Colloid Polym. Sci.* 1996, 274, 197-208.

6. Jay F., Haudin J.M., Monasse B.J.; *Mater. Sci.* 1999, 34, 2089-2102.
8. Aciermo S., Palomba B., Winter H.H., Grizzuti N.; *Rheol. Acta* 2003, 42, 243-250.
9. Elmoumni A., Winter H.H., Waddon A.J.; *Macromolecules* 2003, 36, 6453-6461.
10. Janeschitz-Kriegl H., Ratajski E., Staudlbauer M.; *Rheol. Acta* 2003, 42, 355-364.
11. Watanabe K., Takahashi T., Takimoto J., Koyama K.J.; *Macromol. Sci. Phys.* 2003, B42, 1111-1124.
12. Baert J., Van Puyvelde P.; *Polymer* 2006, 47, 5871-5879.
13. Vleeshouwers S., Meijer H.E.H.; *Rheol. Acta* 1996, 35, 391-399.
14. Pogodina N.V., Winter H.H.; Srinivas S.J.; *Polym. Sci. Polym. Phys.* 1999, 37, 3512-3519.
15. Pogodina N.V., Lavrenko V.P., Srinivas S., Winter H.H.; *Polymer* 2001, 42, 9031-9043.
16. Somani R.H., Yang L., Hsiao B.S., Fruitwala H.J.; *Macromol. Sci. Phys.* 2003, B42, 515-531.
17. Somani R.H., Yang L., Zhu L., Hsiao B.S.; *Polymer* 2005, 46, 8587-8623.
18. Somani R.H., Hsiao B.S., Nogales A., Srinivas S., Tsou A.H., Sics I., Balta-Calleja F.J., Ezquerro T.A.; *Macromolecules* 2000, 33, 9385-9394.
19. Agarwal P.K., Somani R.H., Weng W., Mehta A., Yang L., Ran S., Liu L., Hsiao B.S.; *Macromolecules* 2003, 36, 5226-5235.
20. Eder G., Janeschitz-Kriegl H., Krobath G.; *Colloid Polym. Sci.* 1989, 80, 1-7.
21. Liedauer S., Eder G., Janeschitz-Kriegl H., Jerschow P., Geymayer W.; Ingolic E. *Int. Polym. Proc.* 1993, 8, 236-244.
22. Liedauer S., Eder G., Janeschitz-Kriegl H.; *Int. Polym. Proc.* 1995, 3, 243-250.
23. Jerschow P., Janeschitz-Kriegl H.; *Int. Polym. Proc.* 1997, 12, 72-77.
24. Eder G., Janeschitz-Kriegl H.; In *Materials Science and Technology*; Meijer H.E.H., Eds.; Wiley-VCH: New York, 1997; Vol. 18, Chapter 5.
25. Kumaraswamy G., Verma R.K., Issaian A., Wang P., Kornfield J.A., Yeh F.; Hsiao B.S., Olley R.H.; *Polymer* 2000, 41, 8931-8940.
26. Kumaraswamy G., Verma R.K., Kornfield J.A., Yeh F., Hsiao B.S.; *Macromolecules* 2004, 37, 9005-9017.
27. Langouche F.; *Macromolecules* 2006, 39, 2568-2573.
28. Baert J., Van Puyvelde P., Langouche F.; *Macromolecules* 2006, 39, 9215-9222.
29. Pennings J.P.; Ph. D. Thesis, University of Groningen, 1994.
30. Mykhaylyk O.O., Chambon P., Graham R.S., Fairclough J.P.A., Olmsted P.D., Ryan A.J.; *Macromolecules* 2008, 41, 1901-1904.
31. van Meerveld J., Peters G.W.M., Hütter M.; *Rheol. Acta* 2004, 44, 119-134.
32. Vega J.F., Hristova D.G., Peters G.W.M.; Submitted.

Received 23.05.2008 Reviewed 4.11.2008